Structure of Strongly Charged Polyelectrolyte Solutions

James P. Donley*,†

The Boeing Company, Huntington Beach, California 92647

David R. Heine‡

Sandia National Laboratories, Albuquerque, New Mexico 87185

Received March 28, 2006; Revised Manuscript Received September 9, 2006

ABSTRACT: Molecular dynamics simulation and recent theory are used to examine density correlations in semidilute solutions of highly charged, intrinsically flexible, and hydrophilic polyelectrolytes in low salt. Quantitative comparison with no adjustable parameters is made with recent scattering and osmometry experiments. Agreement is found for the polymer−polymer structure factor at intermediate wavevectors q with varying chain charge fraction f. Theory is also in agreement with simulation and experiment for the osmotic pressure but *not* with $q \to 0$ extrapolations of scattering data that show anomalously large intensities at low q.

1. Introduction

Polyelectrolytes play many important roles in living organisms and technology, and interest in them has increased recently as potential core elements in energy devices such as lithium batteries and hydrogen fuel cells. Studied for decades, these charged polymers have been shown to possess a rich set of properties.[1,2] While theoretical progress on polyelectrolytes has been made in a number of areas,[3,4] two of the important issues that remain concern their liquid structure at semidilute densities when they are strongly charged in low salt.

The first is how the density correlations, as exhibited by the monomer−monomer static structure factor $\hat{S}_{mm}(q)$ at intermediate wavectors q, vary with f, the average fraction of monomers on a chain that are charged. The liquid structure as a function of f at constant semidilute polymer monomer density ρ_m has been examined by Nishida, Kaji, and Kanaya (NKK)[5] and Essafi, Lafuma, and Williams (ELW).[6] Their solutions consisted of the linear, intrinsically flexible, hydrophilic, and randomly charged polymer poly(acrylamide-*co*-sodium-2-acrylamido-2-methylpropanesulfonate), or poly-AMAMPS, with monovalent ions and counterions, in salt-free water. The static scattered intensity $I(q)$ was measured for various f using small-angle X-ray (SAXS) and neutron (SANS) methods. Using SAXS, NKK found that at small f the peak position of $I(q)$, q_{max}, increased with increasing f and obeyed a power law but at larger charge fractions $f \sim 0.4$ appeared to reach an asymptote. ELW extended these measurements to higher f and found that q_{max} was effectively constant for $f > 0.4$. Using SANS, they were also able to extract $\hat{S}_{mm}(q)$ from $I(q)$. They found, at least for the range $0.55 \le f \le 0.81$, that $\hat{S}_{mm}(q)$ was invariant for the intermediate wavevectors measured.

The second is the behavior of $\hat{S}_{mm}(q)$ at low q, including the susceptibility $\hat{S}_{mm}(q \to 0)$. The experimental situation here is less clear, especially with many observations of anomalously large scattering $I(q)$ at small q for semidilute solutions with monovalent counterions[7] in low salt.[1,2,8,9] Theoretical understanding on both these issues has been difficult due to the strong interactions that exist in such highly charged solutions. In this article the recent range optimized, random phase approximation (RO-RPA) theory[10,11] is employed augmented by molecular dynamics (MD) simulations to explore both of these phenomena.

2. Theory and Simulation

2.1. System Models. Two models of polyelectrolytes in solution will be considered in this work. The first model, the primitive, consists of a mixture of identical linear, charged polymers and their dissociated counterions. The scaled site−site potential $\beta u_{kk'}(r)$ is effectively hard-core for distances $r < \sigma_{kk'}$ and is Coulombic, $Z_k Z_{k'} l_B/r$, for larger r. Here, Z_k is the valency of a site of type k, k being either a monomer or counterion, denoted by m and c, respectively. Also, $l_B = \beta e^2/\epsilon$ is the Bjerrum length where e, ϵ, and $\beta \equiv 1/(k_B T)$ are the electron charge, solvent dielectric constant, and inverse thermal energy, respectively. The solvent (water usually) is modeled only implicitly through the dielectric constant ϵ. The chains are hydrophilic so the solvent is modeled as good, and thus there is is no short-range attraction, such as van der Waals, between polymer monomers. The polymer molecules are self-avoiding, freely jointed chains with N_m monomers and average bond length b. In this model $\sigma_{kk'} = \sigma$ for all k and k'. Here, $\sigma = b$. The monomers are all charged so that the effect of changing the chain charge fraction f is done by varying the monomer valency $Z_m \equiv f$ from 0 to 1. The counterions are monovalent so $Z_c = -1$. The density of counterions, ρ_c, is determined by charge neutrality, $Z_m \rho_m + Z_c \rho_c = 0$. The second model, the asymmetric, is the same as the primitive except the sizes of the monomers and counterions are set to be as for the real system.

2.2. Theory. The RO-RPA theory is used here to examine the liquid correlations. This theory has been discussed in detail in Donley et al.,[11] denoted as (I), and compared with other theories[12] for liquid structure of polyelectrolyte solutions. However, a brief description is given here to emphasize some important concepts and approximations.

The intention here is to make comparisons with experiments that measure the static scattering intensity $I(q)$. It can be shown that in the single scattering limit $I(q)$ is equal to the weighted sum of the partial structure factors $\hat{S}_{kk'}(q)$. This function $\hat{S}_{kk'}(q)$ is the Fourier transform of the static density−density correlation function

$$S_{kk'}(\mathbf{r} - \mathbf{r}') = \langle (\hat{\rho}_k(\mathbf{r}) - \rho_k)(\hat{\rho}_{k'}(\mathbf{r}') - \rho_{k'}) \rangle \qquad (1)$$

* Corresponding author. E-mail: jdonley@mailaps.org.
† Present address: Valence4 Technologies, Los Angeles, CA 90025.
‡ Present address: Corning, Inc., Corning, NY 14831.

10.1021/ma0607012 CCC: $33.50
Published on Web 10/26/2006

where $\hat{\rho}_k(\mathbf{r})$ is the microscopic number density of sites of type k at position $\mathbf{r}$, ρ_k being its spatially averaged value, and the brackets denote a thermodynamic average. Equation 1 can be computed in principle using equilibrium statistical mechanics and so connects theory and experiment. It is convenient to split $S_{kk'}(r)$, ($r = |\mathbf{r}|$) into intra- and intermolecular pieces, $\Omega_{kk'}(r)$ and $H_{kk'}(r)$, respectively.

$$S_{kk'}(r) = \Omega_{kk'}(r) + H_{kk'}(r) \tag{2}$$

The function $H_{kk'}(r) = \rho_k\rho_{k'}[g_{kk'}(r) - 1]$, where $g_{kk'}(r)$ is the radial distribution function between sites of type k and k' on different molecules a distance r apart.

The RPA theory gives a relation between $g_{kk'}(r)$, $\Omega_{kk'}(r)$, and the site−site potentials $u_{kk'}(r)$. As a molecular generalization of Debye−Hückel theory, it makes use of a linearization approximation that is strictly valid only for weak potentials.[13] For strongly repulsive molecules the RPA predicts that the radial distribution function is negative at small (or not so small for polyelectrolytes) r even though that function is intrinsically nonnegative. This failure affects the intermediate and long-range behavior of $\hat{S}_{kk'}(q)$ such that, for example, for polyelectrolytes at semidilute densities it predicts that q_{max} varies with density as $\rho_m^{1/3}$, which is weaker than the accepted scaling of $\rho_m^{1/2}$.[11] If the repulsive component of the potential is hard-core with a known finite range σ, one solution to this problem is the optimized RPA (ORPA) technique of Andersen and Chandler.[14] However, polyelectrolyte solutions are dominated by Coulomb interactions which have infinite range. The range optimization remedy to this problem is to notice that a strongly repulsive Coulomb interaction between molecules causes $g(r)$ to be very close to zero in a similar manner as would happen with a hard-core potential. In range optimization then the Coulomb potential is replaced at short to intermediate distances r by a hard-core one with some unknown range σ_{eff}. The RPA theory is then solved using the ORPA technique, and the value of σ_{eff} is adjusted so that it has the smallest value such that $g(r)$ is nonnegative for all distances r. In (I), this range optimization scheme was implemented for rod polymers. It was shown there that one example of the improvement of the theory is that the proper density dependence of q_{max} in the semidilute regime is restored, $q_{max} \sim \rho_m^{1/2}$.[11,15]

With the chain structures and potentials known, the RO-RPA theory can be solved numerically for the radial distribution functions and structure factors using the method described in detail in (I).[16] However, the structure of an intrinsically flexible chain itself depends upon its local environment. For example, it is well-known that in the semidilute regime polyelectrolyte chains contract as the density is increased due to increased interchain screening.[4] Therefore, the $\Omega_{kk'}(r)$'s must be computed along with the intermolecular correlation functions $g_{kk'}(r)$. Here, the "single-chain" theory for $\Omega_{kk'}(r)$ is used,[17−19] which has become the standard approach in liquid-state theory of polymers. The theory involves solving by Monte Carlo simulation the structure of the chain in an effective field $u_{kk'}^{eff}(r)$, which embodies the effects of the other molecules in the liquid. The field itself depends upon $g_{kk'}(r)$, $\Omega_{kk'}(r)$, and $u_{kk'}(r)$, and so the inter- and intramolecular correlations are coupled and must be determined self-consistently. The details of the scheme to solve for $\Omega_{kk'}(r)$ are the same as in Heine et al.,[19] except of course that the RO-RPA theory, rather than PRISM, is used to compute the $g_{kk'}(r)$'s.

While the RO-RPA theory improves correlations between repulsive molecules, its predictions for local correlations between attractive molecules remain at the level of the RPA. It is helpful then to improve correlations between polymers and counterions at short distances by incorporating explicit condensed counterions into the primitive model using the two-state model.[11,20−22] In the two-state model, counterions are divided into two species, free and condensed. The condensed counterions are confined to the surface of the chain but are able to translate along its length. Free counterions roam everywhere else not excluded by the condensed region of motion. Free energy minimization is usually used to determine the fraction of counterions that are condensed, f_{cc}.[20] The justification for the use of this model is that it gives improved estimates for the free energy and presumably then also for the liquid structure. Other evidence for the validity of this model is from MD simulations of strongly charged chains.[23] As an example, in Figure 1 is shown a snapshot of a chain and all counterions within 15b of the backbone. It can be seen that indeed a large proportion of the counterions appear to be confined to the chain surface.

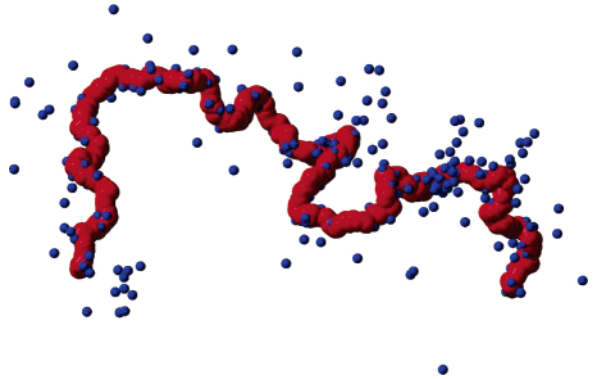

Figure 1. Spatial configuration of atoms from an MD simulation of polyelectrolytes in the asymmetric model at an arbitrary time after equilibration. Shown is a projection onto the simulation box $x-y$ plane of the positions of a single polymer and its neighboring counterions, denoted by red and blue dots, respectively. All counterions within a distance of 15b from the chain backbone are included. Here, $f = 0.8$ and all other conditions are as described in section 3 of the text. As can be seen, a large proportion of the counterions are confined to the chain surface. Note that some clustering of counterions away from the polymer backbone are due to the presence of nearby chains (not shown) since for large f, it is found that $g_{mm}(r)$ rises to 1/2 at around $r = 21b$.

The two-state model was implemented here as in (I) so that the condensed counterions were included as explicit atoms bound to the chain surface.[24] The scheme in summary was to fix the number of condensed counterions per chain, N_c, and with that to compute the correlation functions $g_{kk'}(r)$ and $\Omega_{kk'}(r)$ self-consistently. Then, the free energy was computed using these correlation functions for that fixed value of N_c. Finally, N_c was monotonically increased until a minimum in the free energy was found. As in (I), the implementation was done so as to underestimate the degree of condensation. On the other hand, using the primitive model value for σ_{mc} tends to overestimate the degree of condensation for poly-AMAMPS. This partial balance of approximations should be kept in mind in the comparisons to follow.

2.3. Simulation. The molecular dynamics simulations were conducted using the LAMMPS package for classical systems.[25] Periodic boundary conditions, a particle−particle particle-mesh solver, and a Nose-Hoover (constant *NVT*) thermostat were used. The intermolecular potentials were a sum of a Coulomb and repulsive Lennard-Jones, and the chain bonding potentials were a sum of a FENE and repulsive Lennard-Jones. Further details on the potentials are given elsewhere.[23,26] Integration of the equations of motion was done with a time step $\Delta t = 0.012\tau_{LJ}$,

where τ_{LJ} is the standard Lennard-Jones time. The initial system configuration was a random assembly of charged polymers and counterions. They were then subjected to soft, but large, purely repulsive potentials to straighten the chains and drive the molecules apart. After a very short equilibration period, these potentials were turned off and the true potentials were turned on. Equilibrium was determined by monitoring over time the value of the average polymer end-to-end distance R and the density mode $\hat{S}_{mm}(q)$ for the smallest wavevector $q = 2\pi/L$, where L^3 is the system size. Most simulations were run to time $t_{max} = 2.4 \times 10^4 \tau_{LJ}$, though some at large f were run to $3.0 \times 10^4\ \tau_{LJ}$. Equilibrium was reached at latest at $0.2t_{max}$ for the runs made, which was over 5 times faster than when the Langevin thermostat was used, in approximate agreement with Liao et al.[26] The equilibrium correlation functions $g_{kk'}(r)$, $S_{kk'}(q)$, and $\Omega_{kk'}(r)$ were thus computed using data from times $t > 0.2t_{max}$.

3. Results

In this section comparisons between theory, simulation, and experiment for the monomer−monomer structure factor $\hat{S}_{mm}(q)$ and osmotic pressure Π are shown. Unless stated otherwise, all results for simulation and theory are for conditions of the SANS experiments of ELW on poly-AMAMPS in water. There, b, l_B, and the scaled monomer density $\rho_m b^3$ were 0.25 nm, 0.71 nm, and 0.003, respectively.[6] In the primitive model then, $\sigma =$ 0.25 nm. For poly-AMAMPS with sodium counterions, $\sigma_{mm} =$ 0.53 nm, $\sigma_{cc} = 0.20$ nm, and $\sigma_{mc} \approx (\sigma_{mm} + \sigma_{cc})/2 = 0.37$ nm, so these values were used in the asymmetric model. The chain monomer number N_m has been set to 400 for both theory and simulation, so that this density is well inside the semidilute regime and thus consistent with ELW. The number of polymer chains in the simulation is 100, so density amplitudes are described down to $qb \approx 0.027$.

First, as a test of the theory, the dependence of the intermediate peak wavevector q_{max} as a function of the monomer density ρ_m for fixed f is examined. This intermediate peak can be considered as a measure of the inverse correlation length between polymer monomers.[3] For strongly repulsive polymers (large f here), this length is approximately equal to the size of the correlation hole.[11] It is well-known that determining the semidilute regime for flexible polymers is not straightforward since the chain size varies with the interaction strength which itself varies with density due to screening. As a lower bound on ρ_m then, it is found that for $f > 0.25$ and $\rho_m b^3 \leq 10^{-3}$ the smallest chain size is $R/b = 110$. Modeling the chain as a rod, this size yields a scaled overlap density of $\rho_m b^3 \approx 10^{-4}$. Being conservative then, the density range 10^{-4}−10^{-3} was examined for $f = 0.25$ and $f = 0.75$. It is found that the RO-RPA theory in the primitive model predicts that $q_{max} \sim \rho_m{}^{\nu}$ with $\nu \approx 0.44$ and 0.47 for $f = 0.25$ and $f = 0.75$, respectively, for this density range.[27] As N_m increases and thus the size of the semidilute regime expands, these values approach 0.5. These predictions are then in agreement with results of De Gennes et al.[3] and later theory,[4,18] simulation,[23,26] and experiment.[1,6,28]

Next, in parts A and B of Figure 2 are shown results for the peak position q_{max} and peak height $\hat{S}_{mm}(q_{max})$ of the monomer−monomer partial structure factor, respectively. As can be seen, both the ELW experimental data and the MD simulation predict that both quantities are essentially constant for $f \geq 0.5$. Hence, an explicit modeling of the solvent is not necessary to produce this invariance.

Counterion condensation[21] has been a common explanation for this observed invariance. Condensation theory as developed by Manning is essentially an implementation of the two-state

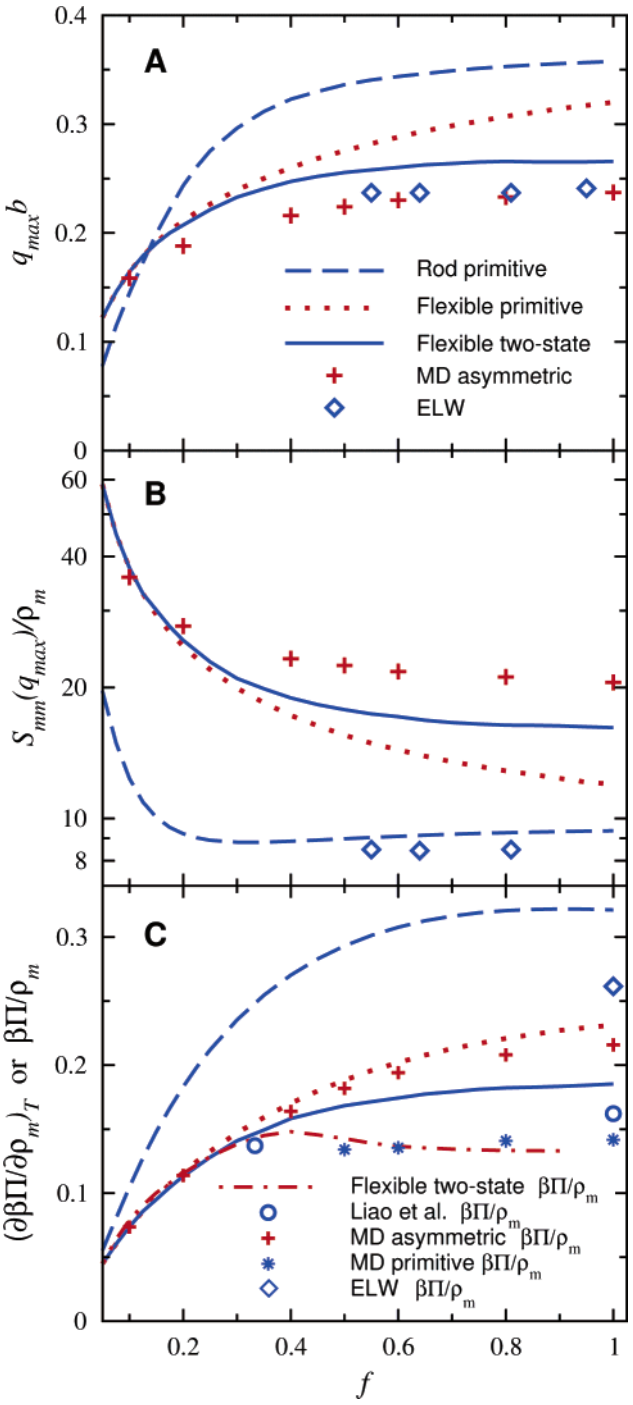

Figure 2. Scaled (A) peak wavevector $q_{max}b$, (B) peak height $\hat{S}_{mm}(q_{max})/\rho_m$, and (C) inverse osmotic susceptibility $\rho_m/\hat{S}_{mm}(0) = (\partial\beta\Pi/\partial\rho_m)_T$ and osmotic pressure $\beta\Pi/\rho_m$ as a function of the average chain charge fraction f. Here, $\rho_m b^3 = 0.003$ and $l_B/b = 2.85$. The meanings of the curves and symbols are shown in the figure legends with those in (A) also applying to (B) and (C). All results are for the RO-RPA theory unless noted otherwise. All data are extracted from the structure factor $\hat{S}_{mm}(q)$ unless noted otherwise. The osmotic pressure data of Liao et al. are for a slightly different condition than that considered here.[29]

model for a single, infinite rod.[21] Manning theory predicts that $f_{cc} = 0$ for $f < f^* = b/l_B$. For $f > f^*$ the strong Coulomb attraction between the rod and counterions causes the counterions to condense onto the rod such as to renormalize f to keep the effective f, $f_{eff} \equiv f - f_{cc}$, constant at f^*. For the poly-AMAMPS systems of NKK and ELW, $f^* = 0.35$, which is consistent with the experimental trends. Extensions of condensation theory to semidilute densities show that many-chain effects

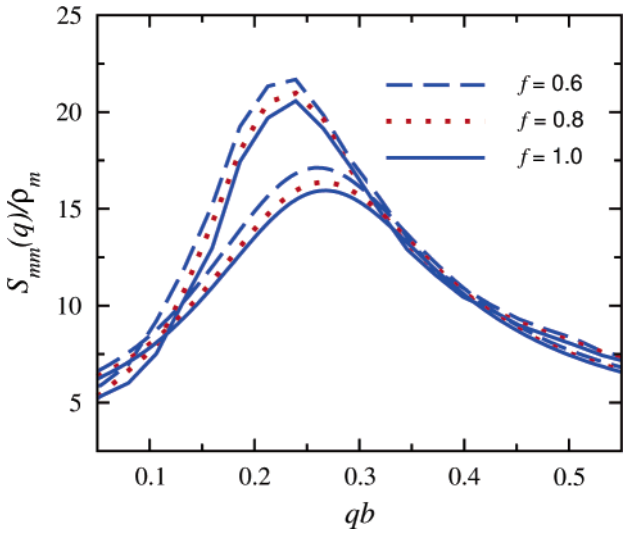

Figure 3. Scaled monomer−monomer structure factor $\hat{S}_{mm}(q)/\rho_m$ as a function of qb for the RO-RPA theory of intrinsically flexible chains in the two-state model (lower block of curves) and MD simulation (upper block of curves) for various charge fractions $f > 0.5$. The conditions are the same as in Figure 2.

round this sharp transition.[20,22] In this picture the invariance arises because repulsions between neighboring chains are dependent on f_{eff}, which remains constant at large f.

To inquire further, results for the RO-RPA in the primitive model for rods are shown. It also predicts that both quantities are invariant at high charge fraction. It has been shown previously that these results are unchanged when the explicit counterions are replaced by a screened Debye−Hückel potential between monomers.[11] Since the only elements remaining in the model then are polymer−polymer repulsions and a diffuse Debye−Hückel screening, a balance between these two effects, and not counterion condensation, is the cause of the invariance. Next, chain flexibility is added. As can be seen, the invariance of both quantities is destroyed: with only Debye−Hückel-like counterion screening the self-repulsion of the polymers causes their chain lengths to increase steadily with increasing f. This elongation in turn causes the repulsion between polymers to decrease and q_{max} to approach the rod values at large f. On the other hand, when condensed counterions are included via the two-state model, this invariance is restored.[30] The observed invariance appears to be mediated partly through the polymer end-to-end distance R, which is found to become constant at large f ($R/b \approx 94$ there for the theory).

As can be seen in Figure 3, the invariance predicted by both the simulation and theory extends to a wide range of wavevectors around q_{max}: from $2q_{max}$ down to about the smallest wavevector measured in the simulation, $q = 0.05/b \approx q_{max}/5$, in approximate agreement with data of ELW.[6]

At large f the quantitative difference for q_{max} between the theory, simulation, and experiment is at most 10%. Combet et al. have shown recently[28] that the scaling predictions of Dobrynin et al.[31] can yield good quantitative agreement for q_{max} at large f if the bare charge fraction in their theory is replaced with f^* from Manning−Oosawa theory. Doing that here yields $q_{max}b \approx 0.295$, which is only about 25% higher than the experimental values. It is possible that the weighting coefficient in the Dobrynin et al. theory, though possibly universal, is not unity, and a more accurate value would yield better predictions. Further experimental comparison would thus be useful. Implementing the same idea for the MD simulation in the asymmetric model and RO-RPA theory gives a value 10% lower and higher, respectively, than experiment.

At small f, NKK have provided evidence that for poly-AMAMPS q_{max} scales with f as a power law, f^n, with $n \approx 1/3$.[5] For hydrophilic polymers, the scaling theory of Dobrynin, Colby, and Rubinstein predicts that $n = 2/7 \approx 0.3$.[31] For the system here for $0.05 \leq f \leq 0.15$, the RO-RPA theory predicts that, if a power law is assumed, then $n \approx 0.4$ and 0.2 for $\rho_m b^3 = 3 \times 10^{-3}$ and 3×10^{-4}, respectively. The RO-RPA results are in good agreement with the results of the MD simulations presented here at least for $\rho_m b^3 = 3 \times 10^{-3}$. For the chain length N_m used here, the size of the semidilute regime is small when f is small. Consequently, this small semidilute regime for small f could account for the variation of n with ρ_m for the RO-RPA theory and for the difference between the RO-RPA theory/MD simulation results and NKK's (and with Dobrynin et al.'s). Further work is ongoing.

The simulation and theory values for $\hat{S}_{mm}(q_{max})$ are in good agreement with each other for all f but are a factor of 2 larger than the ELW values at large f. Comparisons between theory and simulation for polymer melts show that density amplitudes are sensitive to the realism of the molecular model.[33] Using a bead−spring chain model and not incorporating water explicitly could then be considered as the main causes of this discrepancy. However, in the absence of concrete evidence the cause is regarded as unknown, and further study is needed. A less sensitive measure of the strength of polymer−polymer correlations is the scaled full width at half-maximum of $\hat{S}_{mm}(q_{max})$ around q_{max}, $\Delta q/q_{max}$ (with $\Delta q/q_{max} \ll 1$ as the substance becomes crystalline). It is found that, averaged over $f = 0.5$−1.0 ($f = 0.55$, 0.64, and 0.81 for ELW), the agreement for $\Delta q/q_{max}$ between experiment, theory, and simulation is very good, with values 1.38 ± 0.1, 1.36 ± 0.01, and 1.17 ± 0.03, respectively.

Now, does this invariance extend to longer length scales, $q \ll q_{max}$? While computational limitations restrict simulations to intermediate wavevectors ($qb \geq 0.02$ for the density considered here) for the near future, it is a simple matter to solve the theory for much larger system sizes. In Figure 2C is shown

$$\left(\frac{\partial \beta \Pi}{\partial \rho_m}\right)_T = \rho_m / \hat{S}_{mm}(0) \tag{3}$$

as a function of f for various chain types and models. Here, Π is the osmotic pressure on a membrane that is permeable to the salt-free solvent but not to the polymers.[34] As can be seen, a similar picture as for q_{max} and $\hat{S}_{mm}(q_{max})$ emerges. The RO-RPA theory in the primitive model for rods predicts an invariance at large f. Adding chain flexibility destroys the invariance, but adding condensed counterions within the two-state model restores it—though not to as strong a degree as for q_{max} and $\hat{S}_{mm}(q_{max})$.

For long chains in the semidilute regime, $\partial \Pi/\partial \rho_m \approx \Pi/\rho_m$. Also shown then in Figure 2C are results for the scaled osmotic pressure $\beta\Pi/\rho_m$ from theory, simulation, and experiment. The RO-RPA predictions for $\beta\Pi/\rho_m \equiv (1/\rho_m)(\partial \beta F/\partial V)_T$ are computed from the expression for the Helmholtz free energy F.[11] Since the theory is not exact, differences between the theoretical values for $(\partial \beta \Pi/\partial \rho_m)_T$ and $\beta\Pi/\rho_m$ obtained from the structure factor and free energy, respectively, would be expected even if indeed $\beta\Pi \sim \rho_m$.[32] However, it can be seen from Figure 2C that the results between the two thermodynamic routes are in reasonable quantitative agreement, implying that the theoretical predictions are also reasonable for the model used.

CDV

The results above for q_{max} and $\hat{S}_{mm}(q_{max})$ indicate that the theory underestimates the amount of condensation. It would be expected then that the theory's predictions for Π be above those of the asymmetric model simulation; however, it can be seen that that is not so. It is known that a similar optimized theory, PRISM, underestimates the inverse susceptibility for hard-core chain melts, typically by about 25−50%.[33] This behavior then appears to be retained in the RO-RPA at large f, i.e., when the interactions are strong. The agreement between simulation and the osmometry datum of ELW at $f = 1$ is very good considering that the experimental uncertainty is about 10%.[6] Other osmometry data (not shown) for strongly charged polyelectrolytes in the semidilute regime lie in the range $\beta\Pi/\rho_m = 0.15-0.35$[6,35] and so are also consistent with theory and simulation. Also are shown simulation data for the primitive model from the present work and that of Liao et al.[26] These values indicate, as expected, that the condensation and invariance are strongest the smaller is the polymer−counterion contact size σ_{mc}.

Such agreement between theory, simulation, and experiment is interesting because the RO-RPA theory predicts no large density fluctuations for $q < q_{max}$ at these Bjerrum lengths.[11] A large body of experimental data for strongly charged systems similar to that studied by NKK and ELW show a large upturn in $I(q)$ as q decreases below 0.1 nm^{-1} ($qb \approx 0.02$).[2,8,9] This apparent large susceptibility is correlated with dynamic light scattering data that show a slow diffusive mode, i.e., a "slow mode". A common explanation of these measurements is that the polymers have coalesced into clusters of size $R_{cl} \sim 100$ nm $\gg 1/q_{max}$. These clusters are diffuse in the sense that a peak in $I(q)$ remains at q_{max}. There have been many mechanisms offered to explain this phenomenon, counterion-mediated attractions and electro-hydrodynamics being two examples,[1] but no theory to date has provided quantitative predictions.

In the primitive model there is no explicit solvent and hence no hydrodynamics. Further, the RO-RPA, similar to the RPA, captures many-body effects between molecules, apart from those caused by strong repulsive forces, only in a linearized fashion. Thus, the theory is not expected to model well effects such as "counterion-mediated attractions" which are thought to arise from strong attractive correlations.[36] Hence, it is not surprising that the RO-RPA predicts no large scattering at low q that would be due to large clusters. On the other hand, it is surprising then the agreement between the theory and osmometry experiments for Π. A well-characterized set of static scattering experiments for small q is due to Ermi and Amis.[9] Extrapolation of $I(q)$ for their smallest observed wavevectors, $qR_{cl} \sim 1$, to $q = 0$ gives $I(0)/I(q_{max}) = \hat{S}_{mm}(0)/\hat{S}_{mm}(q_{max}) \sim 100$. This value is 100 times larger than that predicted by the RO-RPA theory and therefore that needed to be thermodynamically consistent with the osmometry experiments.

It has been suggested by others that on the time scale of the experiments detailed balance is not achieved for the low q structure of polyelectrolyte solutions.[37] This inconsistency could then be regarded as evidence for this view. Another possibility though is that the low q structure can equilibrate on observable time scales and merely that the extrapolation of the scattering data to $q = 0$ is incorrect. The smallest q's measured have been $\sim 1/R_{cl}$. It can be argued that these wavevectors are not small enough to differentiate a peak at $q \approx 1/R_{cl}$ from a Lorentzian roll-off to a $q = 0$ maximum. Experimental exploration of this issue would be interesting.

4. Summary

In conclusion, a quantitative comparison between theory and experiment for the structure of strongly charged, semidilute polyelectrolyte solutions has been provided. It has been shown that the intermediate length scale structure can be described well by a theory that makes use of the assumptions of equilibrium statistical mechanics. The invariance seen experimentally by NKK and ELW is found to be due to a competition between polymer−polymer repulsions, intrachain repulsions, and counterion screening, the latter being of two types: a diffuse Debye−Hückel and a more local condensed counterion. At longer length scales good agreement is found between theory, simulation, and experiment for the osmotic pressure but not between theory and experiment for the susceptibility. Last, it is argued that more accurate experimental tests of the theoretical relation of eq 3 would help to settle the long-standing question of the origin of the large low q scattering observed in strongly charged polyelectrolyte solutions.

Acknowledgment. We thank David Cannell, Andrey Dobrynin, Wafa Essafi, Bae-Yeun Ha, Wayne Reed, and Marian Sedlak for helpful conversations and correspondence.

References and Notes

(1) Förster, S.; Schmidt, M. *Adv. Polym. Sci.* **1995**, *120*, 52 and references therein.
(2) Sedlak, M. In *Physical Chemistry of Polyelectrolytes, Surfactant Science Series*; Radeva, T., Ed.; Marcel Dekker: New York, 2001; Vol. 99, p 1. Sedlak, M. *J. Chem. Phys.* **2002**, *116*, 5246, 5256.
(3) de Gennes, P.-G.; Pincus, P.; Velasco, R. M.; Brochard, F. *J. Phys. (Paris)* **1976**, *37*, 1461.
(4) Dobrynin, A. V.; Rubinstein, M. *Prog. Polym. Sci.* **2005**, *30*, 1049 and references therein.
(5) Nishida, K.; Kaji, K.; Kanaya, T. *Macromolecules* **1995**, *28*, 2472.
(6) Essafi, W.; Lafuma, F.; Williams, C. E. *Eur. Phys. J. B* **1999**, *9*, 261. Essafi, W.; Lafuma, F.; Baigl, D.; Williams, C. E. *Eur. Phys. Lett.* **2005**,*71*, 938.
(7) For polyelectroltyes in water at room temperature, multivalent ions tend to cause different behavior such as polymer collapse and phase separation. The analyis here then is restricted to solutions with monovalent counterions, the two most common being sodium and chloride.
(8) Matsuoka, H.; Schwahn, D.; Ise, N. *Macromolecules* **1991**, *24*, 4227. Smits, R. G.; Kuil, M. E.; Mandel, M. *Macromolecules* **1994**, *27*, 5599. Wissenburg, P.; Odijk, T.; Cirkel, P.; Mandel, M. *Macromolecules* **1995**, *28*, 2315. Sedlak, M. *J. Chem. Phys.* **1996**, *105*, 10123. Borsali, R.; Nguyen, H.; Pecora, R. *Macromolecules* **1998**, *31*, 1548.
(9) Ermi, B. D.; Amis, E. J. *Macromolecules* **1998**, *31*, 7378.
(10) Donley, J. P.; Heine, D. R.; Wu, D. T. *Phys. Rev. E* **2004**, *70*, 060201-(R).
(11) Donley, J. P.; Heine, D. R.; Wu, D. T. *Macromolecules* **2005**, *38*, 1007.
(12) Laria, D.; Wu, D.; Chandler, D. *J. Chem. Phys.* **1991**, *95*, 4444. Shew, C.-Y.; Yethiraj, A. *J. Chem. Phys.* **1997**, *106*, 5706. Donley, J. P.; Rajasekaran, J. J.; Liu, A. J. *J. Chem. Phys.* **1998**, *109*, 10499. Donley, J. P. *J. Chem. Phys.* **2002**, *116*, 5315; **2004**, *120*, 1661.
(13) Borue, V. Y.; Erukhimovich, I. Y. *Macromolecules* **1988**, *21*, 3240. Joanny, J. F.; Leibler, L. *J. Phys. (Paris)* **1990**, *51*, 545.
(14) Andersen, H. C.; Chandler, D. *J. Chem. Phys.* **1971**, *55*, 1497.
(15) An alternative way to deal with the breakdown of the RPA at short to intermediate distances for the free energy is given in: Ermoshkin, A. V.; Olvera de la Cruz, M. *Macromolecules* **2003**, *36*, 7824.
(16) In eq 14 of (I)[11] the last term should read $\tilde{u}^{sr}_{MkM'k'}(r)$ instead of $\tilde{u}_{MkM'k'}(r)$.
(17) Melenkevitz, J.; Schweizer, K. S.; Curro, J. G. *Macromolecules* **1993**, *26*, 6190.
(18) Yethiraj, A. *J. Chem. Phys.* **1998**, *108*, 1184.
(19) Heine, D.; Wu, D. T.; Curro, J. G.; Grest, G. S. *J. Chem. Phys.* **2003**, *118*, 914.
(20) Gonzalez-Mozuelos, P.; Olvera de la Cruz, M. *J. Chem. Phys.* **1995**, *103* 3145. Solis, F. J.; Olvera de la Cruz, M. *J. Chem. Phys.* **2000**, *112*, 2030.
(21) Manning, G. S. *J. Chem. Phys.* **1969**, *51*, 924. Oosawa, F. *Polyelectrolytes*; Marcel Dekker: New York, 1971.
(22) Nyquist, R. M.; Ha, B.-Y.; Liu, A. J. *Macromolecules* **1999**, *32*, 3481.
(23) Stevens, M. J.; Kremer, K. *J. Chem. Phys.* **1995**, *103*, 1669.
(24) A minor difference between the implementation of the two-state model here and in (I) was that here the condensed counterions were allowed to float smoothly on the chain surface, including exploring any positions between monomers, rather than being allowed only to sit

on the "tops" of monomers. The resulting quantitative change in f_{cc} was at most a few (5) percent.
(25) Plimpton, S. J. *J. Comput. Phys.* **1995**, *117*, 1.
(26) Liao, Q.; Dobrynin, A. V.; Rubinstein, M. *Macromolecules* **2003**, *36*, 3386, 3399.
(27) For low densities, $\rho_m b^3 \ll 10^{-3}$, solving the theory in the explicit two-state model becomes computationally burdensome. However, since the primitive and two-state models become the same at low charge fraction and the two-state acts to make the effective charge fraction a constant at high charge fraction, it is expected that the scaling of q_{max} with ρ_m in the two-state to be the same as the primitive.
(28) Combet, J.; Isel, F.; Rawiso, M.; Boue, F. *Macromolecules* **2005**, *38*, 7456.
(29) The simulation data of Liao et al. for the osmotic pressure shown in Figure 2C are for polymers with solvent neutral backbones in the primitive model with $N_m = 187$, $\rho_m\sigma^3 \approx 0.0015$, $l_B/\sigma = 3.0$, and $b/\sigma \approx 1.1$.[26]
(30) The RO-RPA predicts that $f_{eff} \approx 0.45$ at $f = 1.0$.
(31) Dobrynin, A. V.; Colby, R. H.; Rubinstein, M. *Macromolecules* **1995**, *28*, 1859.
(32) The relevance of the thermodynamic inconsistency problem to the RO-RPA theory is discussed in more detail in (I), section 3.3.
(33) Pütz, M.; Curro, J. G.; Grest, G. S. *J. Chem. Phys.* **2001**, *114*, 2847. Curro, J. G.; Webb, E. B.; Grest, G. S.; Weinhold, J. D.; Pütz, M.; McCoy, J. D. *J. Chem. Phys.* **1999**, *111*, 9073.
(34) Higgins, J. S.; Benoit, H. C. *Polymers and Neutron Scattering*; Clarendon Press: Oxford, 1994.
(35) Wang, L.; Bloomfield, V. A. *Macromolecules* **1990**, *23*, 804 and references therein.
(36) Ha, B.-Y.; Liu, A. J *Phys. Rev. E* **1999**, *60*, 803.
(37) Phillies, G. D. J. *Macromolecules* **2001**, *34*, 8745 and references therein. Michel, R. C.; Reed, W. F. *Biopolymers* **2000**, *53*, 19. Sorci, G. A.; Reed, W. F. *Macromolecules* **2002**, *35*, 5218.

MA0607012